Proceedings of ASME Turbo Expo 2011
GT2011
June 6-10, 2011, Vancouver, British Columbia, Canada

GT2011-45673

INFLUENCE OF UNSTEADY TURBINE FLOW ON THE PERFORMANCE OF AN EXHAUST DIFFUSER

Marcus Kuschel
Institute of Turbomachinery and Fluid Dynamics
Leibniz University Hannover
Appelstr. 9, 30167 Hannover, Germany
kuschel@tfd.uni-hannover.de

Joerg R. Seume
Institute of Turbomachinery and Fluid Dynamics
Leibniz University Hannover,
Appelstr. 9, 30167 Hannover Germany
seume@tfd.uni-hannover.de

ABSTRACT

For the design of highly efficient turbine exhaust diffusers, it is important to take into account the unsteady flow field induced by the last turbine stage. A 1/10 scale model of a gas turbine exhaust diffuser consisting of an annular followed by a conical diffuser is used to investigate the influence of the unsteady flow conditions on the performance of the diffuser. To reproduce the outflow of the last turbine stage, a NACA profiled rotor is placed at the inlet of the diffuser.

Measurements with 3D hot-wire probes are conducted in order to resolve the unsteady flow mechanisms inside the annular diffuser. Additionally, unsteady pressure transducers are installed at the shroud of the diffuser and on the surface of the NACA blades to detect rotating instabilities generated by the rotor.

For operating points with a high flow-coefficient, vortices are generated at the tip of the blades. They support the boundary layer at the shroud with kinetic energy up to the half-length of the annular diffuser, which leads to a high pressure recovery. For operating conditions without generated vortices, the pressure recovery is significantly lower.

The analysis of the pressure signals at the shroud and at the rotating blades with auto- and cross-correlations show that the number of generated vortices at the tip of the blades is lower than the number of blades. For the operating point with the highest flow coefficient, it can be shown that fourteen vortices are generated at the tip of the thirty blades.

In modern RANS-model based CFD-codes, turbulence is modeled as isotropic flow. By comparing the three Reynolds Stress components behind the rotor it can be shown that the flow field especially in the wake of the blades is non-isotropic. This shows that diffuser flows should be modeled with turbulence models which account for non-isotropy.

Keywords: diffuser, hot-wire, vortex, boundary layer, rotating instabilities, isotropy

NOMENCLATURE

AK	auto-correlation
c	$\sqrt{c_{ax}^2 + c_{\tan}^2}$
c_p	pressure recovery factor
h	height
KK	cross-correlation
N	number of samples for averaging
p	pressure
PD	unsteady pressure transducer
r_c	casing radius
r_h	hub radius
T	period for one blade passing
t	time
TKE	turbulent kinetic energy
u	velocity
u’	unsteady velocity in x-direction
$\tilde{u}$	ensemble averaged velocity
$\overline{U}$	averaged mean velocity
v’	unsteady velocity in y-direction
w’	unsteady velocity in z-direction

Subscripts

AD	annular diffuser
ax	axial
Euler	Euler radius
i	velocity component
inlet	inlet of the annular diffuser
j	counter for sample number
out	outlet annular diffuser

stat	static
tan	tangential
tot	total

Greek Symbols

τ	time step in period T
Φ_{xx}	coefficient for auto-correlation
Φ_{xy}	coefficient for cross-correlation

INTRODUCTION

A maximum effort is applied in the development of new turbines to achieve an increase in efficiency. The advancement of turbine exhaust diffusers in terms of a better pressure recovery, reduced losses, and a compact design can contribute to this development. As an example of the impact of an increase in diffuser efficiency, Farhoki [1] identified an about 0.4% benefit in the turbine power generation for a rise of the pressure recovery coefficient of 0.2 for an exhaust diffuser with a realistic inlet Mach number of 0.4. The design of exhaust diffusers is based on extensive charts, which do not take into account the turbulence and swirl in the flow from the upstream turbine, i.e. Sovran and Klomp [2] or ESDU [3]. Due to the need for creating new design charts for exhaust diffusers, which take the unsteady flow characteristic of the upstream turbine into account, the investigation of the impact of unsteady flows on the performance on diffusers was published by many authors.

Sharan [4] demonstrated that beside the geometrical and velocity profile parameters the turbulence intensity in the longitudinal direction is very important for the diffuser performance. Stevens and Williams [5] showed that a fully developed flow in the inlet of an annular diffuser and the associated generated turbulence leads to a higher pressure recovery and reduced total pressure loss compared to a not fully developed velocity profile at the inlet. A further increase of pressure recovery of up to 20% can be achieved by introducing artificial turbulence with only little slightly total pressure loss.

Becker and Stoffel [6] investigated the impact of the compressor flow on the pressure recovery of a downstream aircraft-engine diffuser. The diffuser consists of an annular pre-diffuser followed by a dump diffuser with a liner, which can be varied in its axial position. The compressor flow was replicated by a modelled 1 ½ staged axial compressor, which consists of two rows of inlet guide vanes and a rotating spoke wheel between the vane rows to vary the rotating frequency without influencing the mass flow rate. It was shown, that the pressure recovery increases with the appearance of periodic wakes of the spoke wheel. The changed direction of the wakes with increased rotational speed or the enlarged frequency of the wakes caused the decay of the wakes within the downstream part of the diffuser. The intensity of the wakes was high enough to diffuse into the boundary layer and to stabilize it, which leads to a higher pressure recovery.

Pfeil and Höing [7] investigated the turbulent boundary layer in a diffuser behind an axial compressor. It was shown, that the boundary layer behind the stator blades is three-dimensional in contrast to the boundary layer between to stator blades, which are two-dimensional.

Kruse et al. [8] analyzed the influence of a turbine stage on the performance of annular diffusers with a different hub ratio. The flow from the turbine stage had a significant influence on the performance of the diffuser. The tip clearance and the swirl are mentioned as the factors with the major influence.

Cherry et al. [9] varied in experiments for CFD validation the expansion angle of an annular diffuser section and introduced wake disturbances of three airfoil-shaped struts upstream the diffuser inlet. The 3D velocity measurements are conducted using a Magnetic Resonance Velocimeter. It is shown that the wakes of well-streamlined struts do not lead to local flow separation and have little impact on a diffuser with a conservative expansion angle, which does not stall. The work is the continuation of earlier conducted test cases for CFD-validation. One of them was conducted by Grundmann et al. [10] to investigate the sensitivity of separated flow in a diffuser to inlet condition variations. Plasma actuators are used to introduce streamwise and spanwise forces to the inlet flow, which lead to the generation of different orientated vortices. It was shown that the pressure recovery in the diffuser is very sensitive to the flow inlet conditions in terms of secondary flows. The downstream velocity profile for the conditions with the highest pressure recovery is the least unsteady character.

The three-dimensional characterization of the flow inside an annular exhaust diffuser model including 24 vanes in the inlet was conducted by Ubertini and Desideri [11]. Six struts are installed additionally at the half length of the annular diffuser. The wakes of the inlet vanes contribute to the flow separation at the shroud. Separation at the shroud is detectable between the wakes of the struts and the adjacent inlet vane wake. A rapid growth of the boundary layer and separation at the hub occurs not far behind the strut. The determination of turbulent length scales show that the strut wakes and the separated regions are characterized by small dissipating eddies. In terms of the measured turbulence characteristic the flow between the vanes and the struts is nearly isotropic whereas anisotropy is present behind the struts.

The attached flow field in a two-dimensional straight walled diffuser and the influence of different materials for the side walls was investigated by Mobarak et al. [12]. Amongst other things anisotropy was indicated in the flow, which would lead to an inaccurate application of an isotropic eddy viscosity hypothesis for the simulation of a flow similar to this conditions.

Sieker and Seume [13] [14] investigated stabilizing and destabilizing effects of different rotating spoke wheels on the performance of a model exhaust diffuser by varying the mass flow as well as the rotational speed of the rotor and the half-cone angle of the annular diffuser. For an annular diffuser with an half cone angle of 20° and cylindrical shaped spokes the flow separates for operating points with a swirl number lower than 0.1. For high flow coefficients the boundary layer at the shroud is stabilized, which results in a high pressure recovery.

Using a rotor with NACA0020 shaped blades, the flow separates for all operating points. In an annular diffuser with 15° half cone angle using the NACA rotor, the flow does not separate for operating conditions with a high flow coefficient. The experiments show that the flow field and the performance of the annular diffuser strongly depend on the inlet conditions.

Based on these investigations, the mechanism leading to the stabilizing effects are investigated and presented in this paper for the annular diffuser with 15° half cone angle and the NACA profiled rotor.

TEST STAND

The experiments were conducted at the diffuser test stand, which was built up by Fleige and Riess [15] as a 1/10 scale model of a gas turbine exhaust diffuser. The set up is shown in Fig. 1.

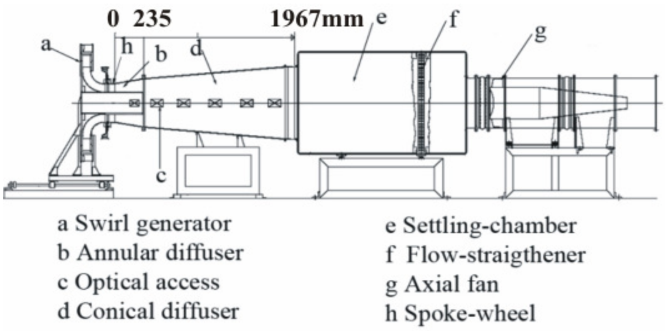

FIGURE 1: DIFFUSER TEST STAND

The axial fan (g) in the rear part sucks the air from the ambient atmosphere through the test stand, so the inlet conditions are not affected by any flow disturbances caused by the fan. The flow enters the test stand radially through the swirl generator (a), which consists of thirty thin metal sheets. These sheets can be bent to apply swirl continuously up to ±35° to the flow. In the presented investigations, no swirl was applied to the flow. After a redirection the flow enters axially the rotating spoke wheel (h) consisting of thirty NACA-0020 profiled blades (Fig. 2). The wakes induced by the blades cause a flow field similar to real turbomachinery. The blade profiles are designed for a mass flow of 5.5 kg/s and 2500 rpm. Further information about the rotor design is given by Sieker and Seume [13]. The rotor is driven by a 4 kW electric motor and the rotational speed can be adjusted continuously up to 3000 rpm. Depending on the operating point it can be operated in a motor or a generator mode to achieve the desired rotational speed.

Behind the spoke wheel the flow enters the diffuser section. The diffuser consists of an annular (b) and a conical part (d). The half cone-angle of the annular diffuser can be varied between 15° and 20°. For the presented investigations the 15° annular diffuser was used, which has an area ratio of 1.78 and a dimensionless length of 2.13 defined as the diffuser length divided by the channel height at the inlet of the diffuser.

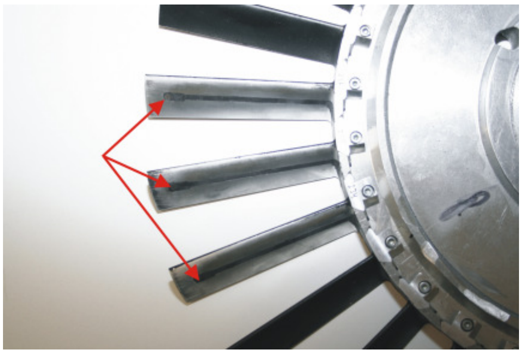

FIGURE 2: PROFILED BLADES WITH UNSTEADY PRESSURE TRANSDUCER (RED ARROWS)

The hub diameter is 140 mm and the outer diameter is 240 mm at the diffuser inlet, which leads to a ratio $r_h/r_c = 0.58$. The local Mach number at the inlet of the annular diffuser is about 0.1 and the Reynolds number is about $4.5 \cdot 10^5$ based on the channel height at the diffuser inlet as characteristic length, which is about one order of magnitude less than for diffusers behind real turbines. At the change-over of the annular diffuser to the conical, the end of the cylindrical hub of the annular diffuser leads to a sudden expansion. The half cone angle of the conical diffuser is 5°. The area ratio of the whole diffuser is equal to 5.2. The investigations in the current paper are focused on the annular diffuser.

Between the conical diffuser and the axial fan a settling chamber (e) with a flow-straightener (f) is installed to achieve homogenous flow field for the axial fan. This fan is driven by a 37 kW motor and continuously adjustable to provide the desired mass flow rate.

INSTRUMENTATION

To measure the distribution of the static and the total pressure in the inlet and the outlet of the annular diffuser, miniaturized three-hole pneumatic pressure probes of cobra type are used. Since the pressure distribution along the channel height can be nonuniform because of swirl and a deviation from the idealized radial equilibrium for some operating points, it is necessary to traverse the probes radially along the channel height. The measured static pressure is area averaged whereas the total pressure is mass flow averaged. The results are used to determine the pressure recovery in the annular diffuser by using the pressure recovery coefficient

$$c_p = \frac{\overline{p}_{stat,out} - \overline{p}_{stat,in}}{\overline{p}_{tot,in} - \overline{p}_{stat,in}}. \qquad (1)$$

The pressure recovery coefficient is defined as the ratio of the static pressure difference between the outlet and the inlet of the annular diffuser to the kinetic energy at the inlet of the diffuser. The axial component as well as the circumferential component is taken into account for determining the static and total pressure. The measurements at the inlet were conducted at a relative axial position l/l_{AD} of 0.08 and at the outlet of 0.95.

The static pressure distribution along the shroud and the hub of the annular diffuser is measured by rows of ten static pressure tabs at two different circumferential positions. To regulate the mass flow, the measurements of two Prandl probes in the radial inlet of the test stand are used. All measured values including the rotational speed of the bladed wheel are reduced to ISO conditions to achieve comparable operating points and measurement results.

The aim of this work is to investigate the unsteady flow mechanisms in the annular diffuser for different inlet conditions, which lead to a different performance of the annular diffuser. The unsteady velocity components are resolved using a DANTEC 55P91 3D hot-wire probe as shown in Fig. 3. The probes are connected to a DANTEC StreamLine frame with an anemometer module for each of the three hot-wires working in the constant temperature mode (CTA). The StreamLine system includes a calibration unit, where the probes are directionally calibrated once as well as velocity calibrated before every use. Since the directional calibration routine of the Dantec system for 3D hot wire probes is not sufficient to generate reliable results, a directional correction procedure has to be implemented. Depending on the flow angle the measured mean velocities have a systematical deviation of maximum 1 m/s, which has no influence on the accuracy of the unsteady velocity components. Additionally, the flow temperature for the calibration as well as for the measurements was recorded to apply a temperature correction to the measured velocities. The measuring frequency was set to 50 kHz, which was tested to be sufficient to resolve the desired flow phenomena.

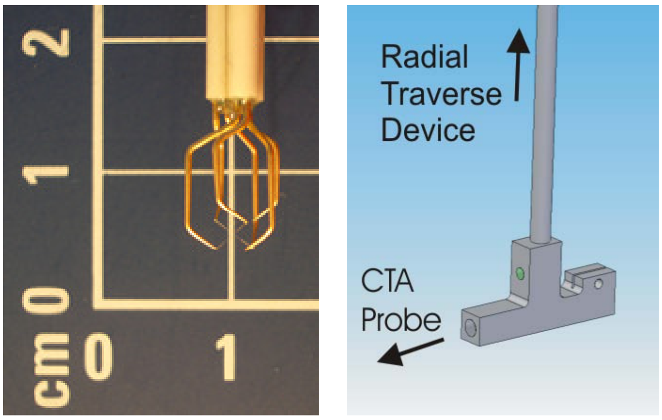

FIGURE 3: 3D HOT-WIRE PROBE AND FIXTURE

A disc, provided with thirty grooves at the circumferential face, is mounted on the shaft, which connects the spoke wheel and the electric motor. While the shaft is turning a hall sensor detects the start and the endpoint of a groove and delivers a TTL-signal, which is recorded for every measurement of the CTA. The angle between two grooves is equal to the angle between two blades. The time between the starting points of two adjacent grooves delivers the time for one blade passing the hot-wire probe which is equal to the period T. The three velocity components u_i measured during this period can be detected and an ensemble averaging of the values can be conducted as described by Griebel and Seume [16]

$$\tilde{u}_i(\tau) = \frac{1}{N}\sum_{j=1}^{N} u_{i,j}(\tau) \tag{2}$$

with τ as time steps for every recorded measurement value within T, N as the number of samples for averaging and u_i as velocity components. N = 400 samples were found to be sufficient to deliver a convergence in the flow statistics. The unsteady velocity components are ensemble averaged as well

$$u'_i(\tau) = \sqrt{\frac{1}{N}\sum_{j=1}^{N}\left(u_{i,j}(\tau) - \tilde{u}_i(\tau)\right)^2} \quad . \tag{3}$$

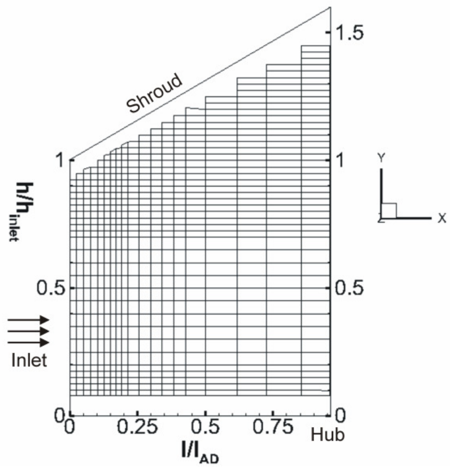

FIGURE 4: GRID FOR CTA MEASUREMENTS IN STREAMWISE DIRECTION

The hot-wire probe is mounted in a fixture (Fig. 3), which makes it possible to adjust the probe continuously in every axial position in the annular diffuser. The fixture is mounted in a radial traversing device. So, it is possible to place the probe in every position in streamwise and radial position of the annular diffuser. Due to its diameter of 6 mm, the probe traversing is limited at the hub and at the casing. The grid of the measuring positions in streamwise direction for the detailed investigated operating points is shown in Fig. 4 with l_{AD} as the length and h_{inlet} as the channel height of the annular diffuser inlet. The grid in the diffuser inlet normal to the axial direction is shown in Fig. 6.

To detect possible vortices rotating in circumferential direction, twelve unsteady pressure transducers with a measurement range of ±350 mbar are installed flush with the shroud surface. They are mounted in four axial sections with three transducers in every section, respectively. The axial sections are placed in the annular diffuser inlet, in the annular diffuser outlet, and two equidistant between them. The arrangement of the transducers in every axial section is shown in Fig. 5. The different angles between the transducers lead to different running distances of the vortices from one transducer to the next, what is important for the following analysis.

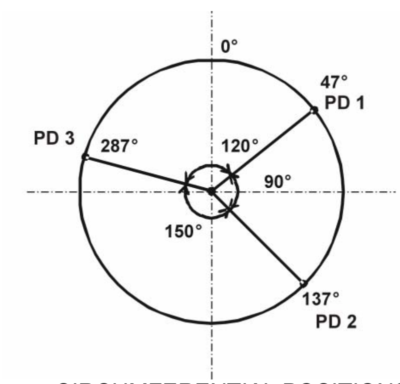

FIGURE 5: CIRCUMFERENTIAL POSITIONS FOR THE PRESSURE TRANSDUCERS (PD) IN FLOW DIRECTION

To determine the number of rotating vortices and the rotating speed, the signals are evaluated by auto-correlations

$$\phi_{xx}(\tau) = \lim_{T\to\infty} \frac{1}{2T} \int_{-T}^{+T} x(t) x(t-\tau) dt . \qquad (4)$$

Here the signals are correlated at one unsteady pressure transducer for different time steps. For the evaluation by cross-correlations

$$\phi_{xy}(\tau) = \lim_{T\to\infty} \frac{1}{2T} \int_{-T}^{+T} x(t) y(t-\tau) dt \qquad (5)$$

the signals of two different pressure transducers are correlated for different time steps. The maximum values from this correlation are used to determine graphically the number and direction of rotating flow instabilities.

Additionally three unsteady pressure transducers are installed flush to the surface at the tip of three adjacent blades of the NACA profiled rotor (Fig. 2). The signals are led through the blades and the shaft and out of the rotating system by a slip ring. The measuring frequency is set to 50 kHz as for the CTA.

TEST PROGRAM

Experiments with seven different operating points were conducted by varying mass flow and rotational speed of the rotor. An overview is given in Tab. 1.

TABLE 1: LIST OF THE EXPERIMENTS

	mass flow [kg/s]	rotational speed of the spoke wheel [rpm]	flow coefficient ϕ [-]	flow angle [°]	tubulence intensity [%]
V1	5.3	2500	0.73	8	4.03
V2	6.3	2500	0.88	-2	4.34
V3	5.3	1500	1.21	-18	5.47
V4	5.5	3000	0.63	11	4.58
V5	4.8	1500	1.1	-16	5.28
V6	6.1	3000	0.7	5	4.20
V7	5.1	2500	0.7	5	4.33

The results of the experiments V1-V3 are presented in more detail in the following sections. The flow coefficient

$$\phi = \frac{\overline{c_{ax}}}{u_{euler}} \qquad (6)$$

is the ratio of the averaged axial velocity in the inlet of the diffuser divided by the circumferential velocity of the rotor at the Euler radius. The turbulence intensity

$$Tu = \frac{1}{\overline{\overline{c_{ax}}}} \sqrt{\frac{1}{3}\left(\overline{u'^2} + \overline{v'^2} + \overline{w'^2}\right)} \qquad (7)$$

is defined as the unsteady velocity component related to the averaged axial velocity. In the inlet of the diffuser, the distribution of the turbulence intensity and the normalized axial velocity over the channel height is nearly constant. Therefore some important integral parameters to describe the flow in the diffuser inlet for the different operating conditions are mentioned in Tab. 1.

RESULTS

In the following sections the results of the experiments are presented in terms of analyzing the inlet conditions, the behavior of the boundary layer at the shroud regarding the influence of the inlet conditions, and the rotating vortices at the shroud. Finally, an assessment is conducted in terms of the isotropy of the flow behind the rotating blades. The axial velocities and the turbulent kinetic energy are normalized by the averaged axial velocity at the diffuser inlet $\bar{U}0, inlet$. The streamwise position l is normalized by the length of the annular diffuser l_{AD}.

Inlet conditions

The inlet conditions strongly affect the development of the flow in the following diffuser. In Fig. 6 to 8 the normalized axial mean velocity at the diffuser inlet behind the rotor is shown for the channel height vs. the period T, which is equal to one blade passing from the left to the right side of the pictures. The lower normalized axial velocity reveals the wake in the middle of the picture.

The normalized axial velocity for V1 is shown in Fig. 6. To make the resolution of the measurement grid normal to the axial direction clear, the grid is added in this figure. In the region close to the hub the wake is more distinctive than in the upper part and the axial velocity at the pressure side of the blade in the right part of the figure is higher than at the suction side and more shroud-sided.

In Fig. 7 the velocity field is shown for V2. The velocity at the pressure side is more shroud-sided than for V1. Especially at the radial height from 0.9 on a region with high axial velocity is detectable over nearly the whole period T. At the tip of the wake a vortex can be detected which an extension from 0.3 to 0.5 of the period T.

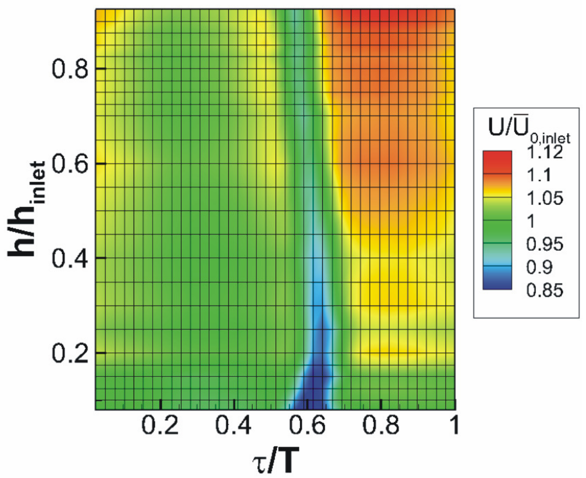

FIGURE 6: NORMALIZED AXIAL MEAN VELOCITY AT THE AXIAL POSITION 0 FOR V1

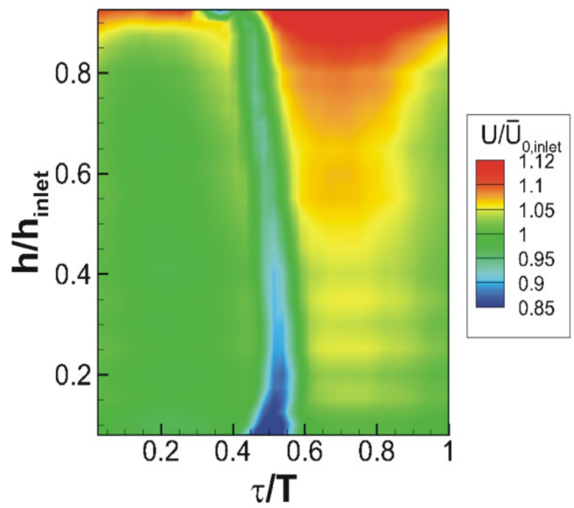

FIGURE 7: NORMALIZED AXIAL MEAN VELOCITY AT THE AXIAL POSITION 0 FOR V2

In Fig. 8 the normalized axial mean velocity for V3 reveals that the vortex at the tip of the wake is more distinctive than for V2. The velocity field is more shroud-sided and the vortex at the tip of the wake is more intensive. The wake especially at a channel height below 0.4 is less intensive than in V1 and V2.

The vortex at the tip of the wake can be detected for V5 as well. That leads to the assumption that this phenomenon arises for operating points with a flow coefficient higher than 0.8.

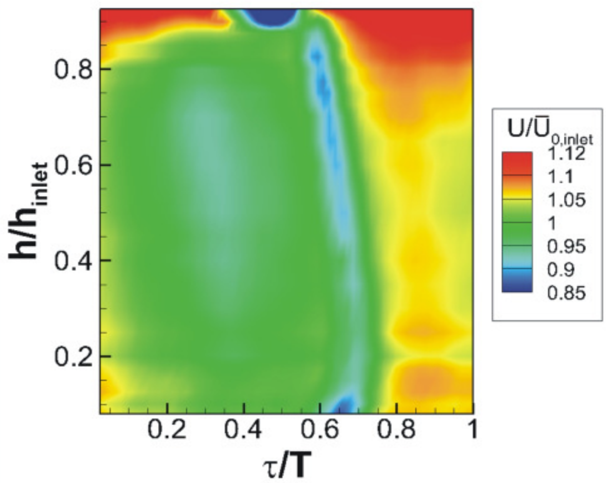

FIGURE 8: NORMALIZED AXIAL MEAN VELOCITY AT THE AXIAL POSITION 0 FOR V3

Many authors [4] [5] [6] [8] [13] [14] explain a higher pressure recovery with increasing turbulent kinetic energy at the inlet of the diffuser. The turbulent kinetic energy normalized by the square of the mean axial velocity at the inlet is defined as followed:

$$\frac{TKE}{\overline{U}^2_{0,inlet}} = \frac{0.5\left(\overline{u'^2} + \overline{v'^2} + \overline{w'^2}\right)}{\overline{U}^2_{0,inlet}}. \tag{8}$$

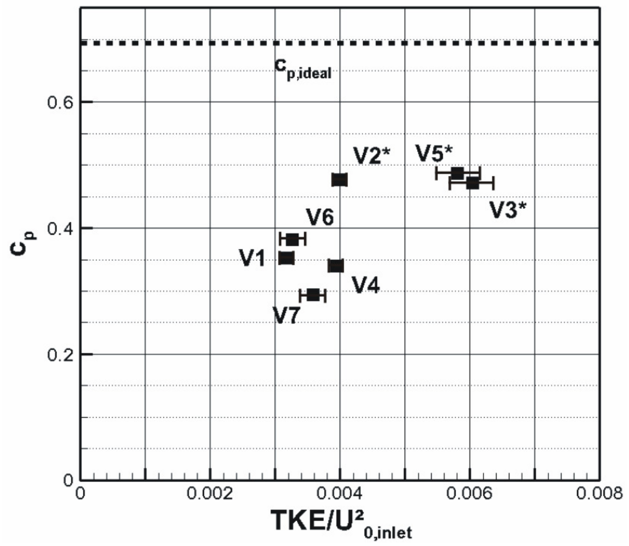

FIGURE 9: PRESSURE RECOVERY VS. NORMALIZED TURBULENT KINETIC ENERGY

In Fig. 9 the pressure recovery related to the normalized integral turbulent kinetic energy in the inlet of the annular diffuser for V1-V7 is shown together with the ideal pressure recovery coefficient

$$c_{p,ideal} = 1 - \frac{1}{AR^2} \tag{9}$$

with a value of 0.69. For six of the seven operating conditions a trend of increasing pressure recovery with higher normalized turbulent kinetic energy can be detected. Only one operating point (V2) reaches a pressure recovery of 0.48 with a normalized turbulent kinetic energy of 0.004. For all operating points with a pressure recovery higher than 0.4, which are marked with a star in Fig. 9, a vortex can be detected at the tip of the wake as described above. Since the three operating points V2, V3, and V5 with the highest flow coefficient lead to the highest pressure recovery, the results in [13] can be confirmed. V3 and V5 have the highest values of integral turbulence intensity (see. Tab. 1). Regarding the vortices at the tip of the profiled blades it can be assumed that the integral turbulent kinetic energy at the inlet is not crucial for a high pressure recovery in general but also where this kinetic energy is induced into the flow to stabilize the boundary layer.

Boundary layer

To achieve a high pressure recovery, it is necessary that the flow channel in the diffuser is not constricted by a growth of the boundary layer in order that the flow decelerates and the static pressure increases. In Fig. 10 the normalized turbulent kinetic energy is shown for the whole length l_{AD} and height h of the annular diffuser and one period T. The wakes induced by the rotor can clearly be detected up to a normalized length of 0.5. The boundary layer at the shroud and the hub grows and leads to a constricted duct for the free flow. The turbulent kinetic energy at the inlet is not sufficient to stabilize the boundary layer against the pressure gradient in streamwise direction. The normalized turbulent kinetic energy increases in the boundary layer due to increasing energy dissipation in this region.

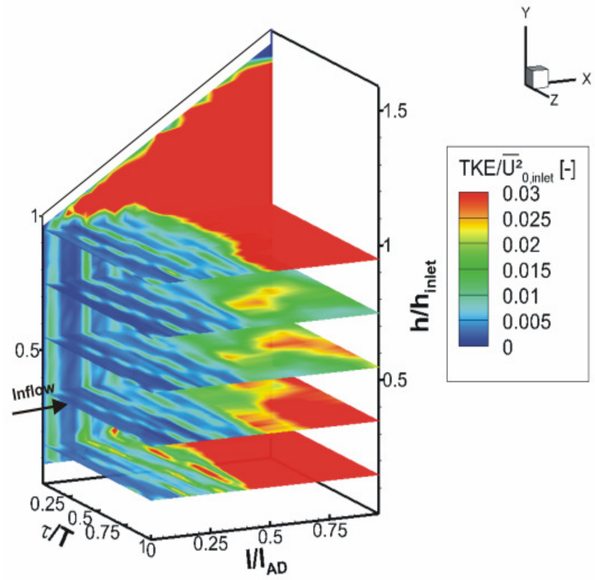

FIGURE 10: NORMALIZED TURBULENT KINETIC ENERGY IN THE ANNULAR DIFFUSER FOR V1

In Fig. 11 the normalized turbulent kinetic energy in the annular diffuser is shown for V2. The boundary layer is not as thick as in V1. The high kinetic energy in the upper part of the inlet induced by the vortices at the tip of the wakes can be clearly identified. The vortices at the tip of the wake can be detected up to a normalized length of 0.4. It can be assumed that these vortices transport kinetic energy into the boundary layer. Therefore the boundary layer can be stabilized against the adverse pressure gradient.

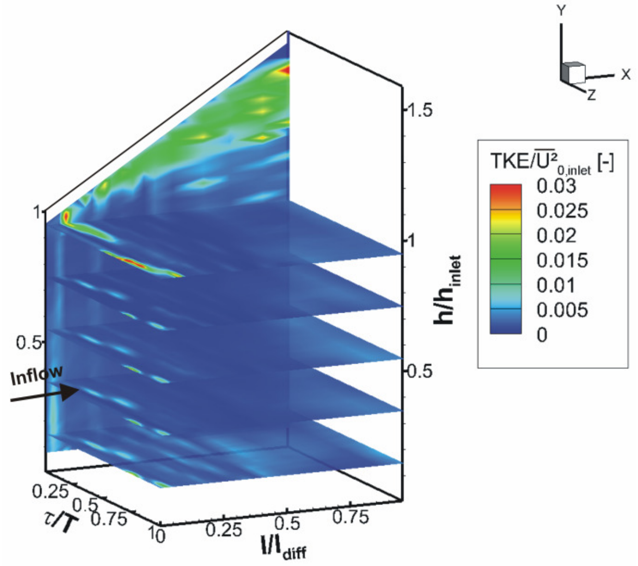

FIGURE 11: NORMALIZED TURBULENT KINETIC ENERGY IN THE ANNULAR DIFFUSER FOR V2

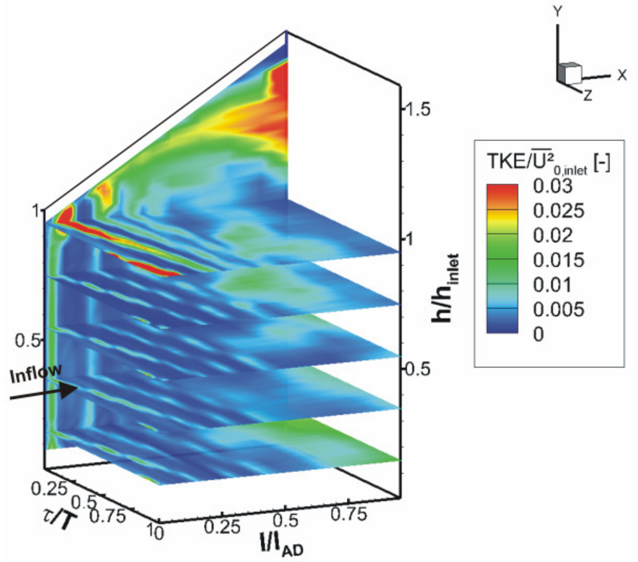

FIGURE 12: NORMALIZED TURBULENT KINETIC ENERGY IN THE ANNULAR DIFFUSER FOR V3

In Fig. 12 the vortices at the tip of the wakes of V3 are more distinctive than for V2. The normalized turbulent kinetic energy in the upper front part of the diffuser is higher than in V2. The size of the vortices is larger as well what may lead to a stronger transport of kinetic energy stabilizing the boundary layer.

The results in Fig. 10 to 12 show that an increasing boundary layer as well as the production of dissipating turbulent kinetic energy are reasons for a decreasing pressure recovery as in V1. A detailed analysis, which cause has a major influence on the decrease in pressure recovery, has to be conducted in further investigations. The results demonstrate the behavior of the boundary layer depending on the turbulent kinetic energy induced by vortices at the inlet of the diffuser and transported into the boundary layer. Since the figures show the ensemble averaged results, it will be shown in the next section, whether these vortices occur at every wake tip or if they are generated at less than thirty blade tips.

Vortex generation

In order to investigate the vortex generation a windowed Fast Fourier Transformation (FFT) is conducted by means of the signals recorded with the CTA. In Fig. 13 the results of this FFT are shown for the whole channel height at an axial length of $l/l_{AD} = 0$ for V3.

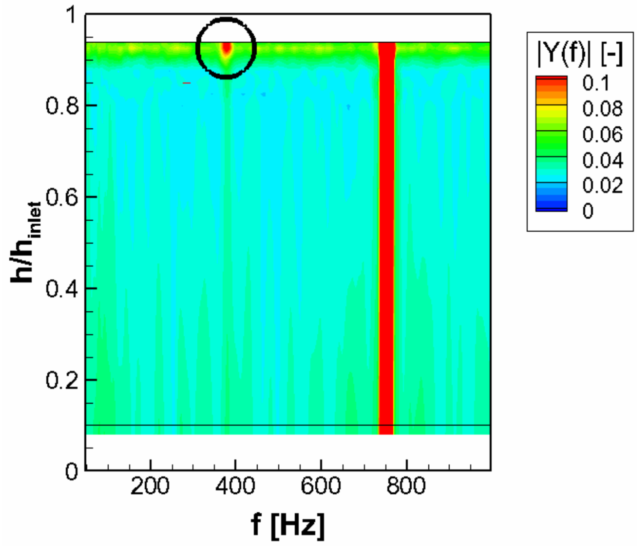

FIGURE 13: FFT ANALYSIS OF THE CTA SIGNALS AT A NORMALIZED AXIAL POSITION L/L_{AD}=0 FOR V3

Beside the blade passing frequency of about 750 Hz, which is visible for the whole channel height, an additional peak can be detected at a frequency of 379 Hz from a normalized radial position on of 0.9 (see the black circle). At lower radial positions this frequency peak is not that strong. It can be assumed that the peak at the top is related to the generated vortices. Since the detected frequency is lower than the blade passing frequency this leads to the assumption, that the vortices are not generated at the tip of every of the thirty blades, but permanently.

To disprove or confirm this theory, the pressure signals of the unsteady pressure transducers in the blades as well as at the shroud in the inlet of the annular diffuser are analyzed in terms of rotating instabilities by auto- and cross-correlations (see Eq. 4 and 5) to identify the number of rotating vortices generated by the rotor. For the unsteady pressure transducers at the shroud a FFT analysis is conducted as well. In the case of V3 the same frequency as in the FFT analysis of the CTA signals of 379 Hz can be detected with a high peak as well.

After applying a low pass filter the auto- and cross-correlation of the signals is conducted.

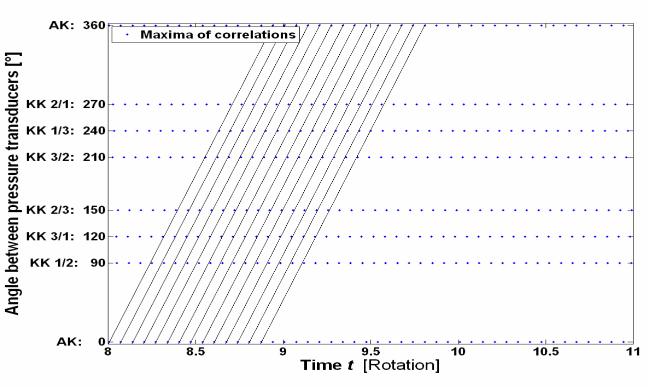

FIGURE 14: NUMBER OF ROTATING INSTABILITIES AT DIFFUSER INLET FOR V3

In Fig. 14 the results of the pressure signal correlations are shown. The auto- (AK) and cross-correlations (KK) for the different angles between the three unsteady pressure transducers are plotted against the time in terms of the rotations of the rotor. The points depict the correlation maxima for the auto- and cross-correlations with respect to the runtime and the angle between the according pressure transducer. By connecting the points a regression line can be determined with a minimum distance between the line and the points. The maxima of the auto-correlations at 0° and 360° are congruent in terms of time. So the end point of the first line on the left at 360° is the start point for the next rotation at 0°. Therefore fourteen lines can be determined in the diagram what leads to fourteen rotating vortices at the shroud. The vortices rotate with 1/0.93 speed of the bladed rotor.

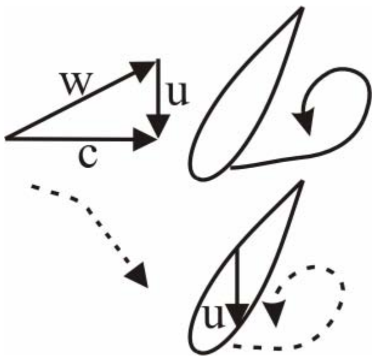

FIGURE 15: GENERATION OF A ROTATING INSTABILITIY AT THE TIP OF A BLADE

The same kind of analysis was conducted for the unsteady pressure transducers implemented in the profiled blades. Since the angles between the profiled blades and between the detected unsteady pressure measurements are 12°, the correlation analysis as in Fig. 14 looks different due to the different runtimes between the transducers. The analysis shows fourteen rotating instabilities, what approves the assumptions derived from the prior analysis.

A possible explanation for the emergence of the vortices is shown in Fig. 15. For high flow coefficients the incidence angle of the flow in the rotating system deviates strongly from the design point. This leads to a flow separation at the pressure side of the blade. Since the passage between these two blades is blocked, the flow is deviated to the next passage in rotating direction. The resulting more disadvantageous incidence angle causes the next blocked passage, while the first one is open again. Hence the resulting vortices move in the rotating direction of the bladed wheel. This explains the higher rotating velocity of the vortices compared to the bladed wheel. Since it is a very dynamic procedure not behind every second blade erases a blockage at the same time and it leads to the fourteen rotating vortices.

The analysis of the rotational instabilities for V1-V2 does not show that clear results as in V3. The FFT analysis for V1-V2 shows in the upper radial positions beside the blade passing frequency another high peak, but the correlation analysis of the unsteady pressure transducers at the shroud as well as in the blades does not allow a clear evaluation as for V3. In terms of the additional frequency peak in the CTA measurements it can be assumed, that not on every blade tip a vortex arises as well, but the exact number can not be determined at this time.

Therefore it is not possible to clear at this time, if the fourteen vortices are related to this rotor or if their number is related to aerodynamical phenomena, which could lead to a different number of rotating vortices. It can be excluded that the fourteen vortices are related to an asymmetry in the blades.

Isotropy

Beside experimental investigations flow fields are simulated with computer fluid dynamics (CFD). Up to now it is still challenging to calculate correctly the unsteady flow field and the pressure recovery in a diffuser with RANS (Reynolds Averaged Navier Stokes) models. Kluß et al. [17] simulated the flow field in the discussed diffuser with a SAS-SST turbulence model and compared it with the experimental results generated by Sieker and Seume [14]. In this work it is shown, that the mixing effects of wakes and secondary flow pattern are responsible for the reattachment of the flow in the annular diffuser. Steady state multistage analyses are not sufficient to calculate the flow field correctly. Therefore unsteady calculations have to be conducted to resolve the physical phenomena of the turbine exit flow and its interaction with the diffuser flow. The RANS model employs the assumption of isotropic turbulence, i.e. the unsteady flow parameters are uniformly distributed in all three dimensions. In Fig. 16 to 18 the Reynolds Stresses are shown for V3 at the axial position $l/l_{AD} = 0$ behind the rotor.

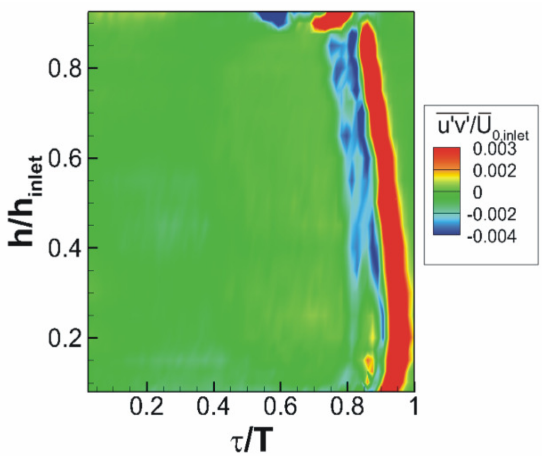

FIGURE 16: REYNOLDS STRESS $u'v'$ FOR V3, AXIAL POSITION L/L_{AD}=0

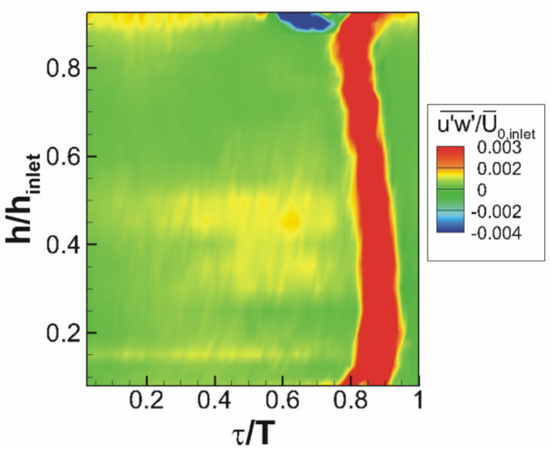

FIGURE 17: REYNOLDS STRESS $u'w'$ FOR V3, AXIAL POSITION L/L_{AD}=0

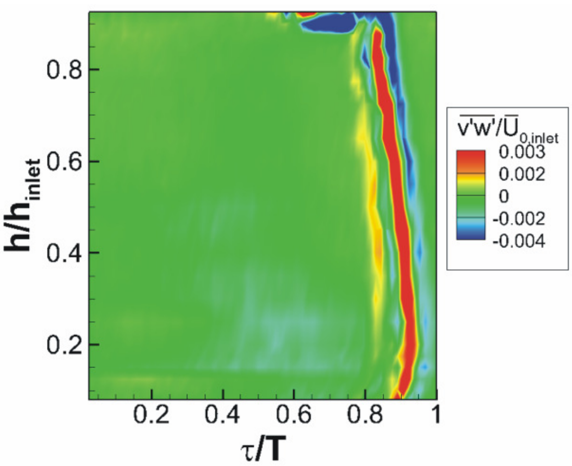

FIGURE 18: REYNOLDS STRESS $v'w'$ FOR V3, AXIAL POSITION L/L_{AD}=0

By comparing these results it can be shown that the flow in the wake is not isotropic, since the Reynolds Stresses are different for every component. These results are approved by other investigations (i. e. Sideridis et al. [18] or Ubertini and Desideri [11]). In the channel between the blades the Reynolds stresses are lower than in the wakes and nearly identical. Since especially the secondary flow mechanism and the wakes have an important influence on the simulation of the flow behaviour in the diffuser [17], it can be concluded that the assumption of isotropic turbulence for the simulations is not correct. The influence on the results can not be estimated here.

CONCLUSIONS AND OUTLOOK

Experimental investigations are conducted to resolve the influence of unsteady flow mechanisms of a rotating stage on the performance of a typical gas-turbine exhaust-diffuser. The diffuser consists of an annular diffuser with a 15° half-cone angle followed by an conical diffuser with a 5° half-cone angle. The measurements were conducted with a 3D hot-wire probe throughout the annular diffuser and with unsteady pressure transducers at the shroud and on the blades of the rotating blades.

For operating conditions with a high flow-coefficient, vortices are detected at the tip of the generated wakes. These vortices, which can be detected up to half the length of the annular diffuser, stabilize the boundary layer at the shroud by transport of kinetic energy into the radial direction. The pressure recovery in the annular diffuser for the operating points in which these vortices occur is significantly higher compared to the operating points without these vortices due to the stabilization of the shroud-side boundary layer.

The investigation of the rotating instabilities at the shroud as well as at the blades of the rotor shows that the number of vortices is lower than the thirty blades of the rotating wheel. This phenomenon is relevant to the CFD simulations of the flow in a diffuser, since it thus is not sufficient to simulate only one blade pitch to resolve this phenomenon.

The flow behind the rotor was additionally investigated such as to assess the applicability of isotropic turbulence in RANS-model based CFD-codes. Especially in the wake behind the rotating blades, the three components of the Reynolds Stresses do not show an isotropic flow field and confirm the results of investigations conducted before. The level of isotropy can be determined by the invariant functions described by Lumley and Newman [19], which is one of the future tasks derived from the results of these experiments. Furthermore, experiments will be conducted with different shaped spokes such as cylindrical spokes with 10 mm diameter and with an annular diffuser with a half-cone angle of 20° to resolve additionally unsteady flow mechanisms which lead to effects stabilizing the boundary layer.

For the design of real turbine diffusers can be derived from these results, that a transport of kinetic energy in terms of vortices into the boundary layer is important to stabilize it. If these vortices have to be generated by the last rotor stage to let them move in circumferential direction at the casing or if it would be sufficient to generate them by a vortex generator fixed to the casing cannot be cleared by these results. If there are more stabilizing effects will be cleared by conduction the experiments mentioned before. All generated results will be compared to derive general, nondimensional approaches for design rules, which are supposed to be applied to real diffuser design.

ACKNOWLEDGMENTS

The investigations were conducted as part of the joint research programme COORETEC-turbo in the frame of AG Turbo. The work was supported by the Bundesministerium für Wirtschaft und Technologie (BMWi) as per resolution of the German Federal Parliament under grant number 0327717B. The authors gratefully acknowledge AG Turbo and MAN Diesel & Turbo for their support and permission to publish this paper. The responsibility for the content lies solely with its authors.

Special thanks to Dr. Alexander Wiedermann and Dr. David Kluß from MAN Diesel & Turbo and the colleagues from the TFD for their support and input and to Fabian Cyris for helping to conduct the experiments.

REFERENCES

[1] Farokhi, S: A Trade-Off Study of Rotor Tip Clearance Flow in a Turbine/Exhaust Diffuser System, ASME Gas Turbine Conference, Anaheim, California, 87-GT-229, 1987

[2] Sovran, G.; Klomp, E.D.: Experimentally Determined Optimum Geometries for Rectilinear Diffusers with Rectangular, Conical or Annular Cross-Section, Fluid Mech. of Int. Flow, Symp., page 270-319, (1967)

[3] ESDU 76027: Introduction to Design and Performance Data for Diffusers, Engineering Science Data Unit, Data Item Number 76027 with Amendment a), London, www.esdu.com, 1990

[4] Sharan, V. KR.: Factors Influencing the Performance of a Diffuser, Indian Journal of Technology, Vol. 14, Feb. 1976, pp. 63-66, 1976

[5] Stevens, S. J.; Williams, G. J.: The Influence of Inlet Conditions on the Performance of Annular Diffusers, Journal of Fluids Engineering, Vol. 102, pp. 357-363, 1980

[6] Becker, B; Stoffel, B.: Experimental investigations of an annular combustion chamber diffuser flow, 17th International Symposium on Airbreathing Engines, ISABE 2005, ISABE-205-1262

[7] Pfeil, H.; Höing, M.: Measurements of the Turbulent Boundary Layer in the Diffuser Behind an Axial Compressor, Journal of Turbomachinery, Vol. 109, pp. 405-412, 1987

[8] Kruse, H; Quest, J.; Scholz, N.: Experimentelle Untersuchungen von Nabendiffusoren hinter Turbinenstufen, MTZ Motortechnische Zeitschrift, Vol. 44, S. 13-17, 1983 (German)

[9] Cherry, E. M.; Elkins, C. J. ; Eaton, J. K.: Geometric sensitivity of three-dimensional separated flows, International Journal of Heat and Fluid Flow, Vol. 29, Issue 03, pp. 803-811, 2008

[10] Grundmann, S.; Sayles, E. L.; Eaton, J. K.: Sensitivity of an asymmetric 3D diffuser to plasma-actuator induced inlet condition perturbations, Experiments in Fluids, Vol. 50, pp. 517-231, 2011

[11] Ubertini, S.; Desideri, U.: Flow development and turbulence length scales within an annular turbine exhaust diffuser, Experimental Thermal and Fluid Science, Vol. 22, pp. 55-70, 2000

[12] Mobarak, A.; Fouad, M. A.; Metwally, M. A.: Turbulence Measurements in a Straight Walled Two Dimensional Diffuser, Gas Turbine Conference, ASME, 86_GT-60, 1986

[13] Sieker, O; Seume, J. R.: Effects of rotating blade wakes on separation and pressure recovery in turbine exhaust diffusers, ASME Turbo Expo 2008: Power for Land, Sea and Air, GT2008-50788, 2008

[14] Sieker, O; Seume, J. R.: Influence of rotating wakes on separation in turbine exhaust diffusers, Journal of Thermal Science, Vol. 17, No. 1, pp. 42-49, 2008

[15] Fleige, H.-U.; Riess, W.: Investigations of gas turbine exhaust diffuser flows, Proceedings of the 4th European Conference on Turbomachinery, ATI-CST-057/01, pp. 665-674, 2001

[16] Griebel, A.; Seume, J. R.: The influence of variable rotor-stator interaction on boundary-layer development in an axial compressor, ASME Turbo Expo 2005: Power for Land, Sea and Air, GT2005-68902

[17] Kluß, D.; Stoff, H.; Wiedermann, A.: Effect of Wakes and Secondary Flow on Re-attachment of Turbine Exit Annular Diffuser Flow, Journal of Turbomachinery, Vol. 131, 041012 pp.1-12, 2009

[18] Sideridis, A.; YYakinthos, K.; Goulas, A.: Turbulence Measurements in the wake of a low-pressure turbine blade, ETTMM8, Volume 1, pp. 86-91, 2010

[19] Lumley, J. L.; Newman, G. R.: The return to isotropy of homogenous turbulence, Journal of fluid mechanics, Vol. 82, part1, pp. 161-178, 1977

